Research on Tremor Suppression Strategies Under a Constant Current Peripheral Electrical Stimulation Device for Parkinson's Disease

Kening Gong, Chuangqiang Guo, *Member, IEEE*, Weihang Guo, Li Jiang, *Member, IEEE*, and Hong Liu, *Member, IEEE*

***Abstract*— Tremor, a prevalent symptom in Parkinson's patients, is conventionally treated with medications and craniotomy. However, the associated side effects and high surgical costs pose challenges for some individuals. In this study, a lightweight constant current electrical stimulator was developed, which is driven by the FPGA to control the underlying logic and has multiple programmable stimulation parameters. Clinical experiments involving patients with Parkinson's-related resting tremor symptoms were conducted to assess the efficacy of peripheral electrical stimulation. Two Co-contraction Avoidance Stimulation (CAS) strategies targeting nerves and muscles were proposed to reduce tremors. Four Parkinson's disease (PD) patients were recruited to verify the effectiveness of these strategies. Kinematic data recorded by inertial sensors showed that the radial nerve and muscle intervention strategies reduced the average angular velocity amplitude of finger joints during resting tremor by 75.92% and 82.41%, respectively. Notably, under low-frequency pulse stimulation (100 Hz) focused on muscle interference, a low-intensity current of no more than 8 mA maintained a tremor suppression rate of 59.91% even 5 minutes post-stimulation. Based on the experimental results, it is concluded that the constant current electrical stimulator developed in this study can effectively suppress tremor under specific stimulation strategies. These findings have significant implications for the development of lightweight, wearable tremor suppression devices. The stimulator's adaptability, coupled with its precise control parameters, demonstrates promise for advancing non-invasive and cost-effective tremor management in Parkinson's patients.**

***Index Terms*— Parkinson's disease, tremor suppression, peripheral electrical stimulation, FPGA, constant current stimulator.**

I. Introduction

PARKINSON'S disease (PD) represents a formidable challenge in neurodegenerative disease management, characterized by a spectrum of motor symptoms that progressively impair movement and quality of life [1], [2]. Among these, the resting tremor, a hallmark symptom of PD, is characterized by involuntary, rhythmic movements primarily affecting the distal limbs. As shown in Fig. 1(a), the pathophysiology of this tremor is believed to originate from the basal ganglia's oscillatory activity, translating into the rhythmic output that drives the alternating contractions seen in patients' hands and wrists [3], [4], [5].

Current clinical strategies for managing PD include pharmacological treatments, with Levodopa-based therapy as the mainstay, and surgical interventions, such as Deep Brain Stimulation (DBS). While Levodopa provides symptomatic relief, its long-term use is associated with diminished efficacy and the onset of dyskinesias [6], [7], [8]. DBS, although effective, is invasive, costly, and not universally accessible [9], [10]. These limitations underscore the urgent need for innovative treatment modalities that are non-invasive, cost-effective, and patient-friendly.

Advances in electronics and robotics have spurred the development of wearable devices for tremor suppression, focusing on exoskeletons and electrical stimulation. Such devices offer a novel approach to managing PD symptoms outside the constraints of traditional clinical settings. Mechanical exoskeletons, targeting the forearm or hand, tend to be physically bulky due to carrying motors or air pumps [11], [12], [13], [14]. Peripheral electrical stimulation, on the other hand, offers a novel approach to managing PD symptoms outside the constraints of traditional clinical settings [15],

Manuscript received 22 March 2024; revised 4 June 2024; accepted 26 July 2024. Date of publication 30 July 2024; date of current version 28 August 2024. This work was supported in part by the National Natural Science Foundation of China under Grant 91948302; in part by Harbin Institute of Technology (HIT) Wuhu Robot Technology Research Institute under Grant HIT-CXY-CMP2-RVJDT-21-01; in part by the Self-Planned Task of State Key Laboratory of Robotics and System, HIT, under Grant SKLRS202112B and Grant SKLRS-2022-ZM-02; and in part by the Foundation for Innovative Research Groups of the National Natural Science Foundation of China under Grant 51521003. *(Corresponding author: Chuangqiang Guo.)*

This work involved human subjects or animals in its research. Approval of all ethical and experimental procedures and protocols was granted by the Ethics Committees of Harbin Institute of Technology under Approval No. HIT-2022023 and the National Center for Neurological Disorders of Capital Medical University under Approval No. KS2022047-1, and performed in line with the Research on the Construction of Parkinson's Disease Cohort and Key Technologies for Diagnosis and Treatment.

Kening Gong, Chuangqiang Guo, Li Jiang, and Hong Liu are with the State Key Laboratory of Robotics and Systems, Harbin Institute of Technology, Harbin, Heilongjiang 150006, China (e-mail: kening.gong@stu.hit.edu.cn; chuangqiang.guo@hit.edu.cn; jiangli01@hit.edu.cn; hong.liu@hit.edu.cn).

Weihang Guo is with the Xuanwu Hospital, Capital Medical University, Beijing 100054, China (e-mail: guoweihang0328@126.com).

Digital Object Identifier 10.1109/TNSRE.2024.3435749

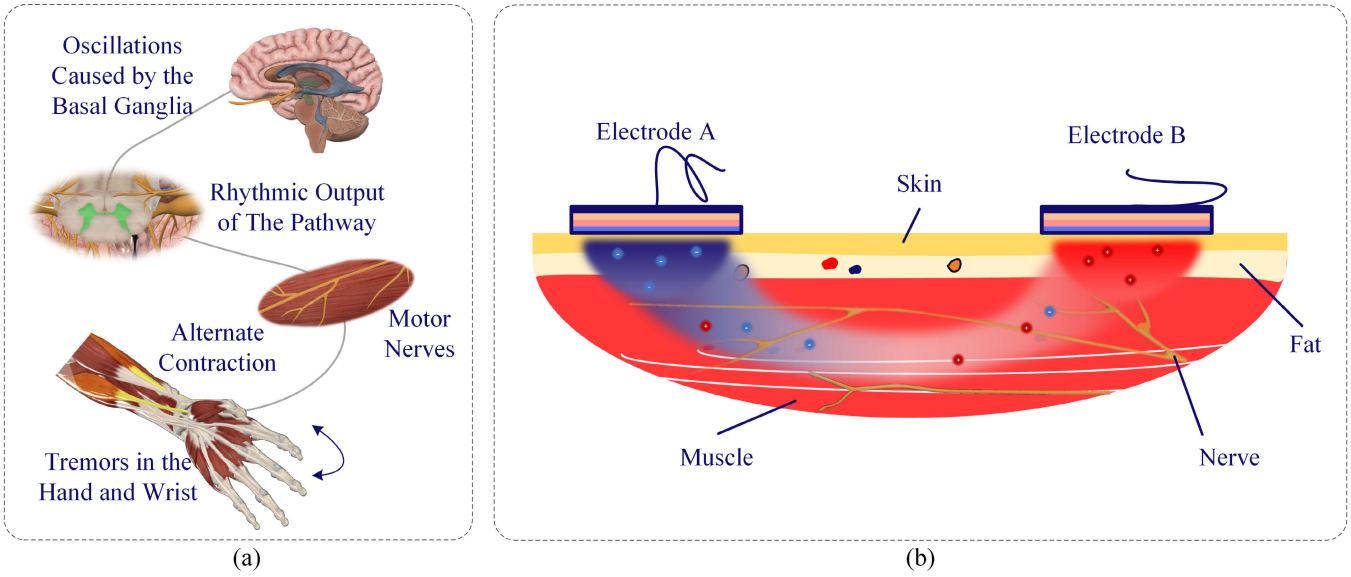

Fig. 1. PD's tremor pathogenesis and peripheral electrical stimulation mechanism. (a) Degeneration in the brain's basal ganglia leads to irregular oscillations. These oscillations disrupt the normal rhythmic output of neuronal pathways, resulting in involuntary, rhythmic muscle contractions and the characteristic tremors observed in the hands and wrists of those with Parkinson's. (b) The electric field generated by non-invasive electrodes placed on the skin prompts a directional migration of ions within the subdermal layers. This movement selectively excites the nerves and muscles below the skin, potentially eliciting action potentials or suppressive signals that could modulate the symptoms or improve motor function in PD patients.

[16], [17], [18], [19]. As depicted in Fig. 1(b), the mechanism of peripheral electrical stimulation operates through the non-invasive application of an external electric field. This field orchestrates the directional movement of ions within the subcutaneous tissues, effectively activating action potentials in both nerves and muscles. This non-invasive technique that is gaining traction due to its potential for in-home use and its capacity for personalized treatment regimens [20].

Peripheral electrical stimulation can be administered through two main avenues: Functional Electrical Stimulation (FES) and Transcutaneous Electrical Nerve Stimulation (TENS). FES directly targets the antagonist muscles of tremor-affected muscles, encouraging a counteracting muscle response [21], [22], [23], [24]. However, this may results in significant muscle stiffness and discomfort, similar to the effects of myotonia, which is counterproductive for long-term patient comfort and treatment adherence. On the other hand, TENS operates below the Motor Threshold (MT), modulating nerve activity without causing muscle contractions, thereby offering a more comfortable and sustainable option for patients [25], [26].

Despite the potential of these techniques, there remains considerable variability in their application, with an absence of standardized protocols for stimulation parameters [22]. This variability hinders the ability to compare and reproduce study results across different research endeavors. In response to this challenge, this study seeks to introduce a systematized approach to tremor suppression using peripheral electrical stimulation.

In this context, we have engineered a wearable device powered by a constant current electrical stimulator that is meticulously controlled by a Field-Programmable Gate Array (FPGA). This stimulator is designed to deliver precise electrical pulses, with adjustable parameters to accommodate individual patient needs and varying physiological conditions. Our study introduces Co-contraction Avoidance Stimulation (CAS) Techniques, which encompass two distinct but complementary strategies designed to suppress tremor without inducing the simultaneous contraction of antagonistic muscle groups. This approach is pivotal for enhancing patient comfort and maximizing the efficacy of tremor management. We conducted a series of experiments with patients exhibiting the characteristic resting tremors of PD, utilizing peripheral electrical stimulation on the radial sensory nerves and antagonistic muscles. The tremor suppression efficacy was quantitatively evaluated using high-precision inertial sensors, and the data was analyzed to discern the benefits of the stimulation strategies.

Our findings show that our stimulator, using a strategy targeting the radial muscles with pulse currents below 8mA, achieved an average tremor suppression rate of 82.41%. Moreover, patients reported no sensations of rigidity or damping during stimulation. This research contributes to the hardware and strategy for peripheral electrical stimulation, with substantial implications for the development of wearable tremor suppression devices.

II. Method

A. Design of Electrical Stimulator

Fig. 2 (a) shows the experimental verification version of the stimulator independently developed by the research team. This device measures 96mm × 73mm × 16mm and weighs 105g (including a 1500mAh battery), demonstrating its potential as a wearable device due to its compact size and lightweight design. This version has two independent electrode channels. The electrical stimulator uses Zynq 7000 SoC

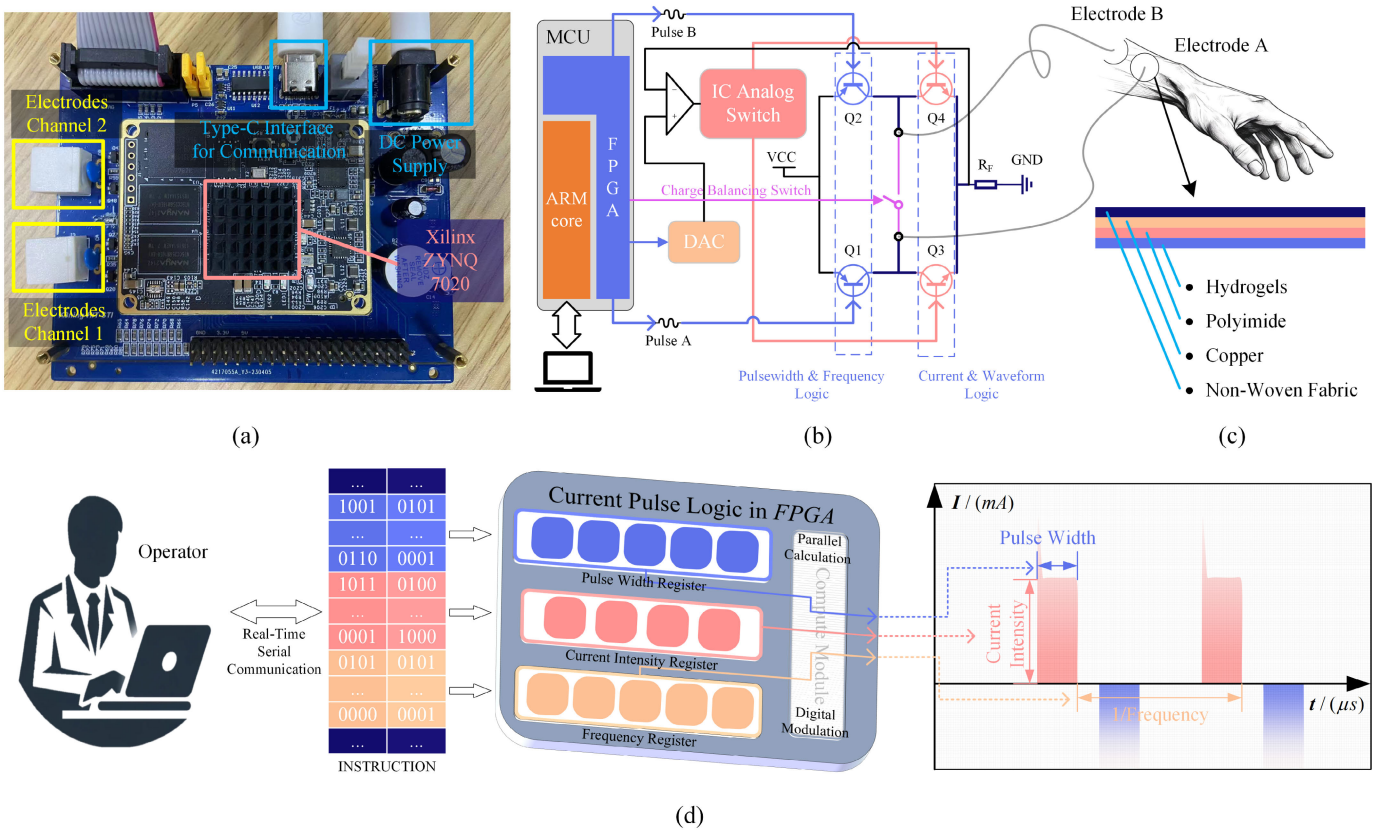

Fig. 2. Electrical stimulator system solution for tremor management. Serial communication between the electrical stimulator and PC is established at a baud rate of 115,200. This facilitates the real-time reception of stimulation parameters by the stimulator, allowing for prompt modulation of the stimulation pulse, leveraging the computational efficiency of the FPGA.

(Zynq Z-7020, Xilinx, US) as the processor, and uses the FPGA module inside the chip to implement the underlying driving logic of electrical stimulation. The ARM unit mainly performs instruction sending and receiving and data processing. The Type-C interface of the electrical stimulator implements two-way communication with the PC through the universal asynchronous receiver-transmitter (UART) protocol, which is used to receive instructions in real time and transmit electrical stimulation parameters back, making it easier to process and control variables during clinical experiments.

The electric stimulator, designed for applications like tremor suppression in PD, incorporates a direct current (DC) interface for its power supply, accommodating a wide input voltage range of 6 ∼ 12V. It employs a boost topology circuit to elevate the voltage to the required range for stimulation. The device's design includes an H-bridge circuit for each electrode channel to guarantee safety and precise current control, as shown in Fig. 2(b). Independent conduction logic for the H-bridge's four transistors ensures accurate parameter settings and stimulation safety. Utilizing the FPGA's high-speed parallel processing capabilities, the pulse width and frequency for each channel are independently adjusted. The H-bridge output circuit not only ensures reverse output capability but also facilitates convenient channel expansion. The stimulator's pulse width is finely tunable from 0 ∼ 510 us in 2us increments. Safety features include independent switches for charge balancing across electrode channels, and current levels are adjustable from 0 ∼ 60 mA. The FPGA precisely regulates stimulation intensity via an SPI-connected DAC (AD5601) and a current feedback circuit, swiftly engaging charge balance post-pulse.

Use a flexible printed circuit board (FPC) to make the stimulation electrode, and the electrode patch is a circle with a diameter of 25 mm, as shown in Fig. 2 (c). FPC electrode sheets are mainly composed of polyimide (PI) and copper foil. In order to facilitate the patient's comfort during the experiment, non-woven fabrics and hydrogel are used to bond the FPC electrode pads. The hydrogel helps increase the humidity on the surface of the patch to improve conductivity. It can also fill in the unevenness of the skin surface, making the electrical stimulation more uniform and effective [27].

Preliminary evaluation of an electrical stimulator's responsiveness and constant current capabilities requires extensive testing. In order to ensure the safety of the test, we established a resistor and a capacitor in parallel between the electrodes as a simulated load, which is similar to the impedance of the human skin surface. By employing a controlled variable method, we meticulously tested the stimulator's responsiveness at pulse widths from 0 ∼ 510 us, frequencies from 1 ∼ 255 Hz, and currents from 0 ∼ 60 mA. In addition, in order to evaluate the constant current output of the stimulator under various loads, we tested resistive loads from 500Ω to 5kΩ under the common parameters of peripheral electrical stimulation of 20mA current, 200us pulse width, and 100Hz frequency.

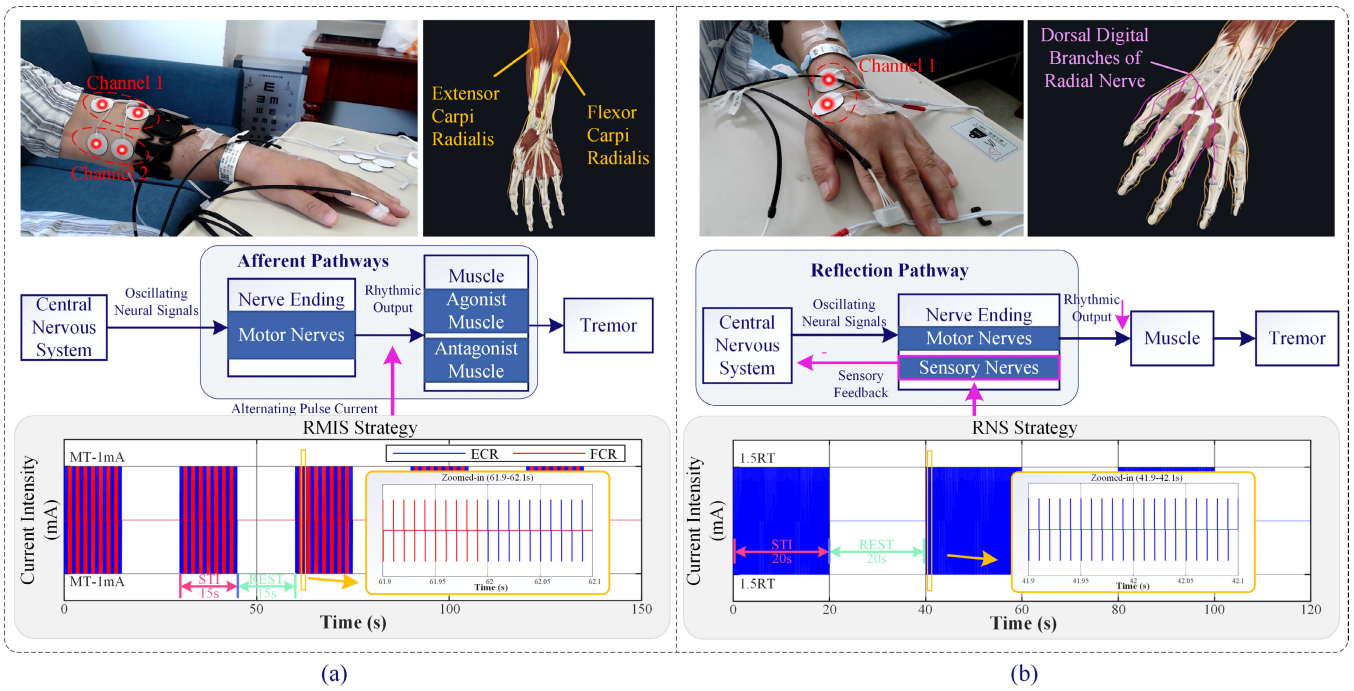

(a) (b)

Fig. 3. Locations and strategies for stimulation. (a) Pulse current below MT acts alternately on FCR and ECR. (b) Pulse current intermittently activates the sensation of the superficial branch of the radial nerve in PD patients.

After testing under simulated load conditions was completed, the study further recruited healthy participants for human trials of the electrical stimulation device under common stimulation parameters. During the testing process, we utilized an Agilent InfiniiVision 3000 DSO-X 3024A oscilloscope to record the voltage waveforms between the electrodes and employed a highly sensitive current clamp (N2893A, Keysight®, US) to accurately monitor the output current of the electrodes. Stimulation results using human forearm skin as a load were recorded to verify the output capability of the electrical stimulator.

B. Stimulation Strategies for Tremor Suppression

Two Co-contraction Avoidance Stimulation strategies were proposed in the experiment. One primarily explores whether the sensory nerve reflex caused by electrical stimulation can inhibit tremor, and the other investigates whether electrical stimulation can alter muscle response to motor neurons to inhibit tremor. Both strategies follow the following principles:

1) Avoid direct muscle contraction caused by electrical stimulation.

2) Avoid electrical stimulation of agonist and antagonist muscles at the same time.

3) Use the lowest possible current intensity to reduce or avoid the subject's discomfort.

The former stimulation strategy (see Fig. 3(a)), which we called Refined Motor Intervention Stimulation (RMIS), mainly stimulated the flexor carpi radialis (FCR) and extensor carpi radialis (ECR) muscles of the patient's arm. This method used a stimulating current to disrupt the motor neurons' efferent signals, thereby altering the muscles' response to the efferent nerves' rhythmic output. RMIS utilized timed alternating stimulation of the FCR and ECR to avoid muscle co-contraction, with the current intensity set to 1 mA below the motor threshold (MT), which varied from 3 to 8 mA depending on the individual. MT is the minimum current intensity that causes muscle contraction. Specifically, the stimulation parameters included a frequency of 100 Hz and a pulse width of 300 μs.

Initial experiments employed a 1 Hz alternating stimulation frequency between the FCR and ECR muscles. This low-frequency parameter was chosen to explore the effects of asynchronous muscle activation on tremor suppression without inducing co-contraction. This frequency was intentionally selected to avoid synchronization with the typical 3-8 Hz tremor frequency observed in Parkinson's disease patients.

The second stimulation strategy, Radial Nerve Stimulation (RNS), was designed to enhance the excitability of the radial sensory nerve in PD patients and to investigate its efficacy in eliciting reflexes within the nerve center to alleviate tremors. As depicted in Fig. 3(b), considering that resting tremors predominantly manifest on the radial side of PD patients' hands [28], [29], electrodes were strategically positioned on the skin overlying the area where the superficial branch of the radial nerve enters the dorsal digital branches. Similar to TENS, this strategy aims to affect sensory nerves, thus avoiding direct muscle contractions. When the electrode is positioned at the branching point of the superficial branch of the radial nerve to the dorsal digital nerve branches, the current is incrementally increased until it evokes a spreading sensation from the back of the hand to the fingers. This spreading sensation, at the current intensity termed the Radiation Threshold (RT), marks the point at which electrical stimulation effectively activates the sensory pathways without

causing muscle contractions. This RT is critical for fine-tuning stimulation intensity, ensuring the activation of sensory neurons without causing discomfort or muscle contractions. The sensory feedback elicited at the RT can engage central neural mechanisms that contribute to tremor suppression [17], [25]. The current intensity was then progressively increased to within the patient's tolerance, from RT to about 1.5 times the RT, to intensify the electrical stimulation's activation of the sensory neurons in the radial dorsal digital branches.

The stimulation protocols for RMIS and RNS were designed with specific durations and cycles to balance effectiveness and patient comfort. For RMIS, the stimulation duration was set to 15 seconds with 15 seconds of rest, repeated over five cycles. This timing was chosen to provide sufficient recovery time for the muscles, minimizing the risk of fatigue and maintaining effective tremor suppression.

For RNS, the stimulation duration was set to 20 seconds with 20 seconds of rest, repeated over three cycles. This slightly longer duration was intended to enhance the activation of the sensory pathways and provide more prolonged tremor suppression effects. The number of cycles was adjusted to ensure patient comfort and avoid overstimulation.

C. Clinical Trials of Stimulation

This study received ethical approval from both the Ethics Committees of Harbin Institute of Technology (ethical approval number HIT-2022023) and the National Center for Neurological Disorders of Capital Medical University (ethical approval number KS2022047-1), securing consent from all participants beforehand. Participants were briefed on the study's objectives, risks, benefits, data handling, electrical stimulation procedures, and data privacy. Four volunteers, aged 48 to 82 (3 males, 1 female), with tremors unalleviated by medication, were selected as participants.

Acknowledging the prevalence of resting tremor in Parkinson's disease primarily in the radial fingers and wrists, this study utilized an inertial measurement unit (IMU) sensor (JY901S, Wit-motion®, CHN) to capture the patient's kinematic data in real-time. Capable of transmitting three-axis acceleration and angular velocity data via serial port, the sensor's sampling rate was set to 100Hz. This rate exceeds the 4∼8Hz frequency commonly associated with resting tremors [30], adhering to the signal sampling theorem. The lightweight sensor, at just 0.97g, connected to the host computer through four 26AWG flexible wires, shielded by a flexible mesh tube to minimize interference with hand movement. As illustrated in Fig. 4, three sensors were affixed to the patient's fingers, the back of the hand, and the wrist—areas most affected by tremor—using medical anti-allergic tape to monitor joint oscillations. A webcam (StreamCam, Logi®, Swiss) recorded the electrical stimulation experiment, with footage stored on a PC.

After being briefed on the experimental procedures by the researcher, the recruited Parkinson's Disease (PD) patients comfortably seated themselves and positioned the arm experiencing tremors on the table. Each patient underwent electrical stimulation trials employing both the RMIS and RNS strategies to ensure a controlled study environment.

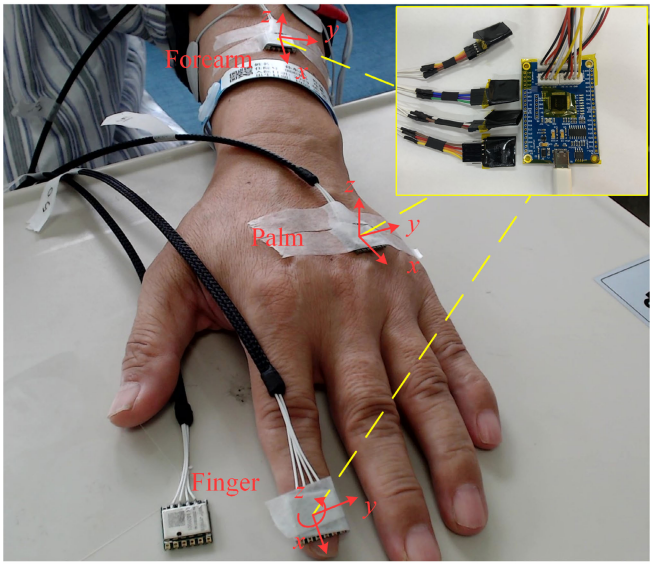

Fig. 4. Distribution of tremor detection sensors on patients' hands. The data parallel acquisition module equipped with FT4232HL transmits data from three IMUs to the computer in real time, recording the kinematic data of the distal interphalangeal joint (DIP), the carpometacarpal joint (CMC), and the forearm.

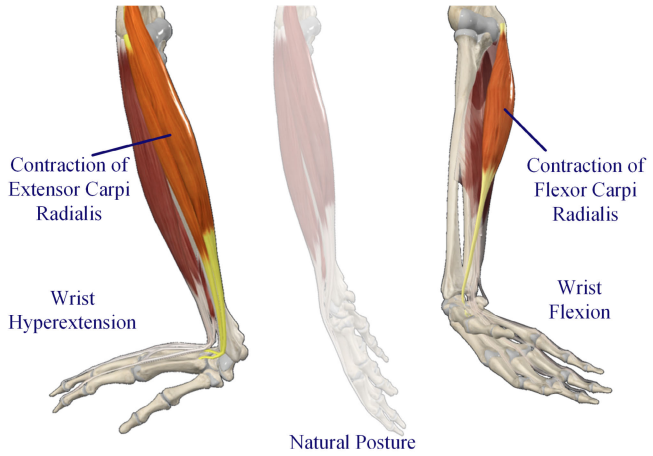

Fig. 5. Specified actions to locate target muscle bellies in PD patients. The patient's wrist hyperextended and flexed, causing the FCR and ECR to contract, helping the researchers quickly determine the location of their muscle bellies.

Preliminary procedures were executed to pinpoint the target muscles and nerves accurately, facilitating precise electrode positioning. The IMUs were strategically placed to ensure accurate recording of the tremor characteristics in these key areas, allowing us to differentiate between various types of tremors and their amplitudes. The IMUs were placed at the DIP, CMC, and forearm to monitor the amplitude and frequency differences of tremors across different joints. The gyroscopes within the IMUs have an internal reference coordinate system, and their orientation was deliberately arranged. This setup ensures that the z-axis data reflect rotational movements around the limb axis, the y-axis data reflect flexion and extension of the joints, and the x-axis data reflect abduction and adduction of the joints.

Before the RMIS experiments, shown in Fig. 5, participants performed wrist movements to help locate the ECR and FCR

TABLE I
PATIENT CHARACTERISTICS AND STIMULATION PARAMETERS

Patient ID	Gender	Age	Tremor Type	Tremor Side	RT (mA)	MT (mA)		RNS		RMIS		
						FCR	ECR	Current (mA)	Protocol	Current (mA)		Protocol
										ECR	FCR	
PD1	Male	64	RT	Left	4	5	5	6		4	4	
PD2	Female	82	RT	Both	4^{R}	6^{R}	5^{R}	6		5	4	
					5^{L}	8^{L}	8^{L}	7	20s / trail 3 times	7	7	15s / trail 5 times
PD3	Male	48	PT	Left	8	9	8	12		8	7	
PD4	Male	61	RT	Right	12	6	4	18		5	3	

muscles. Electrodes were then aligned with muscle fibers on the ECR and FCR. To address individual electrical current sensitivities, the motor threshold (MT) was determined for each patient. The team gradually increased the stimulation current in 1 mA increments, using palpation and observation to identify each patient's MT. In the RMIS trials, stimulation frequency and pulse width were set at 100 Hz and 300 μs, aligning with typical clinical standards [17], [26]. Current intensity was customized based on pre-determined stimulation thresholds. The protocol alternated between 15 seconds of stimulation and rest, repeated over five cycles, to ensure a balanced stimulation approach and to minimize potential muscle fatigue. This approach was intended to balance effective tremor suppression with maintaining muscle integrity and participant comfort.

During the RNS trials, patient feedback was used to determine the optimal stimulation site and the Radiation Threshold (RT) of the radial nerve, with the electrode placed on the radial wrist. The current was increased in 1 mA increments until a spreading sensation from the back of the hand to the fingers was felt, indicating RT. If no radiating sensation occurred, electrode placement was adjusted to more effectively stimulate the radial nerve's superficial branch. Once RT was achieved, the intensity was incrementally raised, with careful consideration of patient comfort, to a target of 1.5 times the RT for the official RNS test. The stimulation protocol consisted of alternating 20-second periods of stimulation with 20-second rest intervals, repeated three times to reduce discomfort. Table I presents the demographics and stimulation settings for all participants.

D. Data Processing and Analysis

The raw data capturing the hand tremors of PD patients were recorded on a laptop (Lenovo®desktop Legion Y9000X, Windows 11) using a program developed in C++. For these tremor measurements, angular velocity data from the IMUs was prioritized over acceleration data due to its lessened susceptibility to changes in the patient's posture and gravitational influences [31]. Each set of recorded kinematic data was timestamped to align with the system clock, ensuring compatibility and comparability across various devices and sensors.

Wavelet analysis was employed to dissect the time-frequency aspects of PD patients' tremor data, focusing on hand position variations. This approach helped identify tremor amplitudes directly from the sensor data. To effectively quantify and compare tremor severity across different experimental stages, data were categorized into five distinct phases: pre-stimulation, during RNS, five minutes post-RNS, during RMIS, and five minutes post-RMIS. During the pre-stimulation phase, participants were instructed to sit quietly with their hands resting on a table for a duration of five minutes. This baseline period was essential for capturing the natural tremor activity without any external intervention. Welch's Power Spectral Density (PSD) estimation was applied to the kinematic data from four patients at these stages, calculating the frequency in Hertz. The Tremor Suppression Ratio (TSR) for each patient was then derived from peak Welch PSD data, both before and after electrical stimulation, as delineated in equations (1) and (2),

$$TSR = \frac{\sqrt{P_{MAX}^{orig}} - \sqrt{P_{MAX}^{sti}}}{\sqrt{P_{MAX}^{sti}}} \times 100\% \tag{1}$$

$$A(f_{peak}) = \sqrt{P(f_{peak})} \tag{2}$$

where A(f_{peak}) represents the amplitude at the peak frequency of the signal, while P_{peak} refers to the peak power of the PSD, indicating the square of the time series raw tremor data per unit frequency. Specifically, when using angular velocity as the metric for describing tremor data, the unit of P_{peak} can be expressed as the square of degrees per second (deg^2/s^2) per unit frequency. The P_{peak} can be calculated as equation (3),

$$P_{peak} = 10^{\left(PSD_{peak}(dB)/10\right)} \tag{3}$$

In the formula, PSD_{peak} represents the peak value of the PSD, expressed in decibels per hertz (dB/Hz). Thus, the TSR quantifies the reduction in the peak frequency's angular velocity before and after electrical stimulation, reflecting the effectiveness of the stimulation in attenuating tremor symptoms.

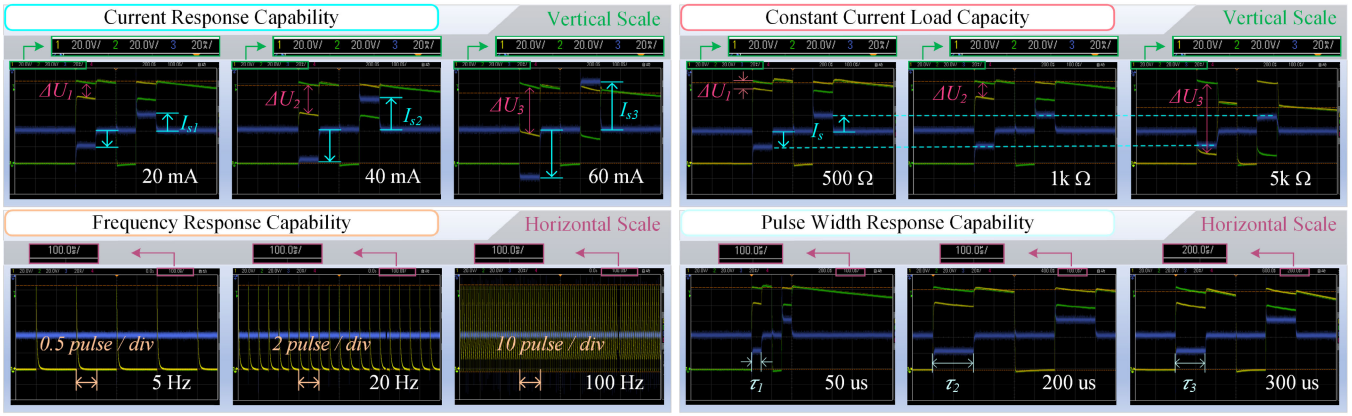

(a)

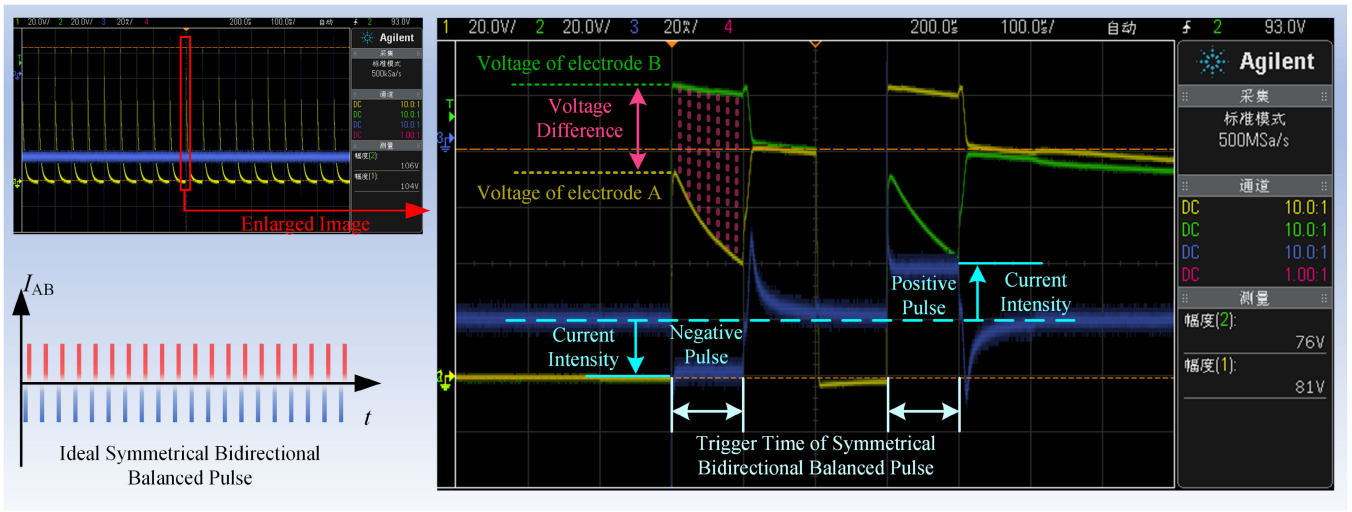

(b)

Fig. 6. Parameter response capability of constant current electric stimulator to generate symmetrical bidirectional pulses. The oscilloscope shows the voltage difference between the two electrodes of the electrical stimulator (yellow and green curves), and the corresponding current intensity (blue curve).

III. Result

A. Design of Electrical Stimulator

Prior to human trials, tests under simulated impedance are conducted to confirm the stimulator's operation within safe limits. Oscilloscope screenshots in Fig. 6(a) illustrate the stimulator's performance across various currents, pulse widths, frequencies, and constant current loads during testing.

During the current response capability evaluation, the stimulator precisely managed stimulation intensity with a minimum increment of 0.25mA, equating to 0.4% of its full current range. This was assessed within the clinically relevant range of 0∼60 mA. With a stable pulse current, the stimulator's output error remained within 0.256mA (±10%), aligning with the clinical standards for minimum step size in electrical stimulation testing, thereby confirming its suitability for clinical application. Pulse width and frequency response tests revealed the stimulator's ability to generate output conforming to specifications within a 0∼510us pulse width and a 1∼255Hz frequency range, with a minimum pulse width increment of 2us. This indicates the device's precise control over output pulse width and frequency, catering to diverse therapeutic requirements. The constant current load capacity was assessed to evaluate the electrical stimulator's performance across various resistances (500 Ω to 5 kΩ), mirroring the typical surface impedance range of human skin. Oscilloscope readings confirmed that current levels were maintained within the preset current size of 20mA ± 1.25%. The above results show that the stimulator can deliver pulse currents with the parameter accuracy needed under simulated impedance conditions, prior to human testing.

Fig. 6(b) presents the impedance response curve of human forearm skin at settings of 20Hz, 200us, and 20mA that are acceptable to the subject. The current curve, captured by a current clamp, reveals that the electrical stimulator can generate the anticipated current with symmetrical bidirectional balanced pulses, even under the impedance conditions of the human body. The oscilloscope data reveal that human skin exhibits complex impedance characteristics, blending resistive and capacitive properties. This complexity results in a capacitor-like charging and discharging behavior at the start and finish of each pulse, highlighting the nuanced electrical

TABLE II
COMPARISON WITH COMMERCIAL PRODUCTS

Feature	Our Stimulator	Master-9 Stimulator (AMPI®, ISR)	RHS Stim/Recording System (Intan Technologies®, US)	DS8R Isolated Bipolar Constant Current Stimulator (Digitimer®, UK)
Isolator / Amplifier	Integrated	ISO-Flex	RHS2116 amplifier chips	Integrated
Current Range	0~60 mA (in 0.25mA steps)	0~10 mA	10 nA ~ 2.55 mA	0~1000 mA
Maximum Output Voltage	110V	90V	14V	120V
Frequency	0~255 Hz (in 1Hz steps)	0~25 kHz	0~20KHz	0~10kHz
Pulse Duration	0~510 μs (in 2μs steps)	40 μs ~ 3999s	(in 2μs steps)	50~2000 μs
Interface	USB (type-C)	USB (type-B)	USB (type-A)	USB (type-B)
Maximum number of channels	2	9	16	1
Weight	105g	5kg (approx.)	\	4kg (approx.)
Power Supply	DC. 6~12V	AC. 110/230 V, 50/60 Hz	AC. 110/230 V, 50/60 Hz	AC. 100V, 120V, 200V or 240V, 47-63Hz

nature of human skin. The voltage difference between the two electrodes continued to increase during the 200us pulse time, indicating that capacitive charge accumulation occurred in the skin and subcutaneous tissue. After the end, the voltage difference between the two electrodes quickly returned to zero within 20us, which showed that the charge balance switch in the electrical stimulator was working effectively. Furthermore, it's noted that during the stable phase of current intensity, the electrical stimulator accurately achieves the preset current levels (target value ± 0.25mA), even when human body impedance acts as the load. This precision helps prevent excessive stimulation or potential skin damage, ensuring the safety and effectiveness of the treatment.

To evaluate the performance of our dual-channel constant current stimulator, we compared its specifications with those of commercially available stimulators. Table II presents a comparison of key parameters such as frequency range, amplitude range, pulse width, and channel count. While our stimulator is limited to two channels, it offers competitive accuracy in frequency and amplitude control, demonstrating its potential for targeted tremor suppression.

B. Original Tremor Characteristics

The kinematic data captured by the IMU sensor offers a more quantifiable and descriptive analysis of the tremor characteristics in patients, as observed by researchers during the experiment. Fig. 7(a) presents the raw tremor data from a PD patient prior to electrical stimulation. During the recording of this data, the patient was instructed to sit quietly with their hands resting on a table to ensure that the tremor data reflected natural resting tremors without any voluntary movements. The angular velocity data across the x-, y-, and z-axis from the patient's fingertips, back of the hand, and arm provides insight into the tremor dynamics at the distal interphalangeal joint (DIP), the carpometacarpal joint (CMC), and the forearm, respectively.

The angular velocity data corresponding to the DIP joint indicate that tremors are primarily distributed along the y- and z-axes, reflecting periodic flexing and adduction movements in the fingers of Parkinson's disease patients during resting tremors, as determined by the orientation of the mounted IMU sensor. Correspondingly, the main components of tremor signals for the CMC joint and forearm are concentrated on the z-axis and x-axis, respectively, indicating radial deviation at the CMC and pronation/supination movements in the forearm. In fact, when the RMS of tremor peaks for both the CMC and forearm do not exceed 10deg/s, the subtle tremor movements become difficult to detect visually. In terms of tremor amplitude, time-domain signals reveal that the statistical peak angular velocity component of the DIP (RMS: 100.24 deg/s) is significantly higher than that of the CMC (RMS: 31.77 deg/s, $P < 2.4e\text{-}19$) and forearm (RMS: 40.93 deg/s, $p < 6.2e\text{-}19$), indicating that tremors in the fingers, especially at the DIP joint, have a greater amplitude and are thus more easily monitored.

The wavelet transform provides a more intuitive representation of the time-frequency characteristics of the patient's original tremor signal, as shown in Fig. 7(b). Excluding the cone of influence area where boundary effects could have an impact, tremor signals from the DIP, CMC, and forearm all exhibit distinct dominant frequency bands. The tremor frequency for each area remains relatively stable, approximately within the range of 3.49Hz ±10%, highlighting a certain degree of consistency ($p > 0.8274$) in tremor frequency across different parts.

The onset of tremors varies significantly among patients, with the primary differences being in the frequency and amplitude of the tremors across individuals. Notably, after conducting wavelet analysis, the tremor signal of each PD patient displays a relatively stable frequency bandwidth, with the statistical outcomes presented in Table III. The findings indicate that the predominant tremor frequency in PD patients ranges between 3 and 9 Hz, and there are substantial

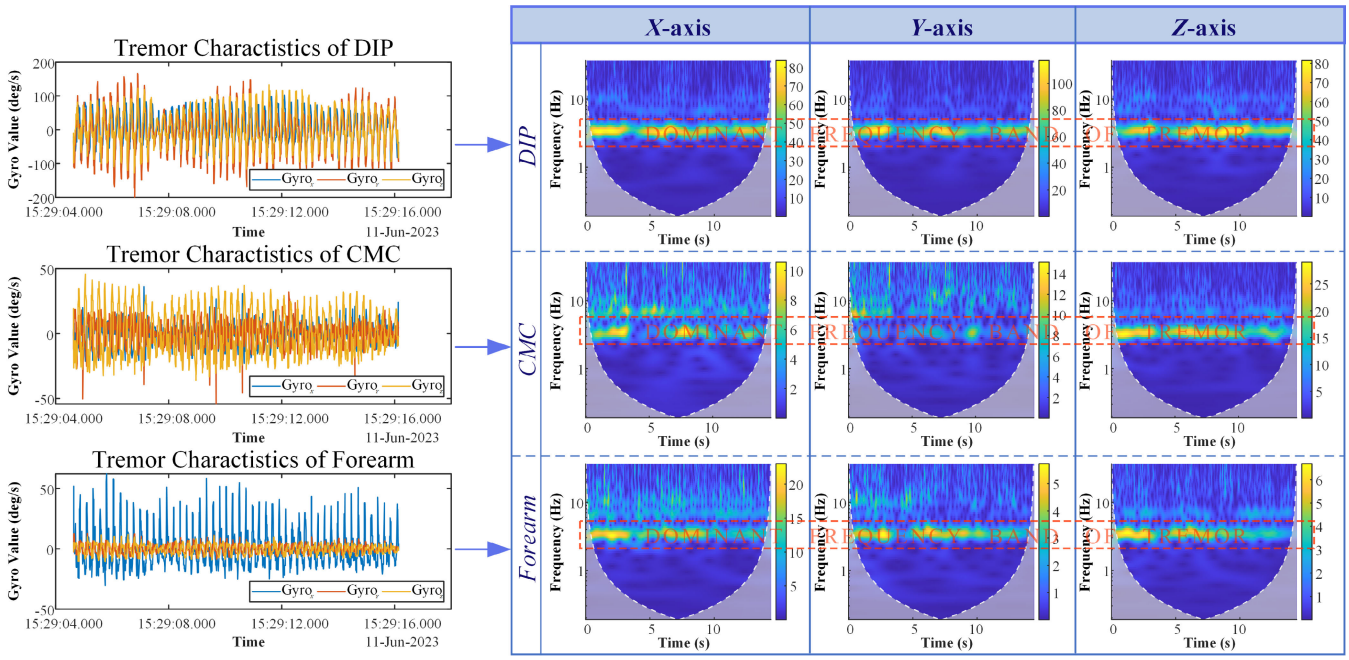

(a) (b)

Fig. 7. Original tremor data and frequency characteristics of PD patients before stimulation. The time-frequency characteristics of the original tremor kinematic data were extracted through wavelet analysis, with the frequency domain being represented on a logarithmic scale.

TABLE III
COMPARISON OF TREMOR AMPLITUDE IN PATIENTS

		PD1 ^{L}	PD2 ^{L}	PD2 ^{R}	PD3 ^{L}	PD4 ^{R}
DIP	Frequency (Hz)	4.60	3.49	3.26	6.51	8.01
	Magnitude (deg/s)	33.71	106.82	50.88	17.36	17.73
CMC	Frequency (Hz)	4.60	3.49	3.26	7.47	7.48
	Magnitude (deg/s)	18.82	25.56	5.78	4.89	5.10
Forearm	Frequency (Hz)	4.60	3.26	3.26	6.51	8.59
	Magnitude (deg/s)	15.87	22.96	1.87	7.34	7.73

differences in tremor manifestations between the two sides of the body. Even among patients experiencing bilateral tremors, there's a marked discrepancy in the tremor amplitude between the left and right hands. Specifically, PD patients with higher tremor frequencies (6∼8Hz) tend to exhibit lower tremor amplitudes at the DIP joint compared to those with lower frequencies (3∼6Hz) ($p < 0.00085$).

C. Efficiency in Tremor Suppression

To quantitatively assess the severity of tremors in PD patients across different stages, power spectral density (PSD) estimation was performed on the kinematic data of four patients at different stages. Fig. 8(a) shows the tremor spectrum data estimated by PSD of Patient PD2's left hand before and after the two electrical stimulation strategies. The peak value obtained based on the PSD estimation can effectively describe the amplitude-frequency characteristics of the main component of the hand tremor signal.

Before receiving electrical stimulation, the PSD analysis indicated that the frequency of the patient's PD2 hand resting tremor signal was Dominant Frequency of 3.32 Hz, and the amplitude of the dominant peak in PSD is 38.13 dB/Hz. During the RNS process, the frequency of the tremor angular velocity was 3.13 Hz, and the amplitude dropped to 27.32 dB/Hz. There is an attenuation of close to 10dB, which represents that the power of the tremor is reduced by half, indicating that electrical stimulation of the radial sensory nerve has an inhibitory effect on this patient's tremor. Five minutes post-RNS, the tremor frequency returned to 3.32 Hz, but the amplitude was slightly reduced to about 34.43 dB/Hz, still lower than pre-stimulation levels. In the RMIS phase, the tremor frequency remained relatively stable at 2.93Hz, yet the amplitude of the dominant peak in PSD significantly

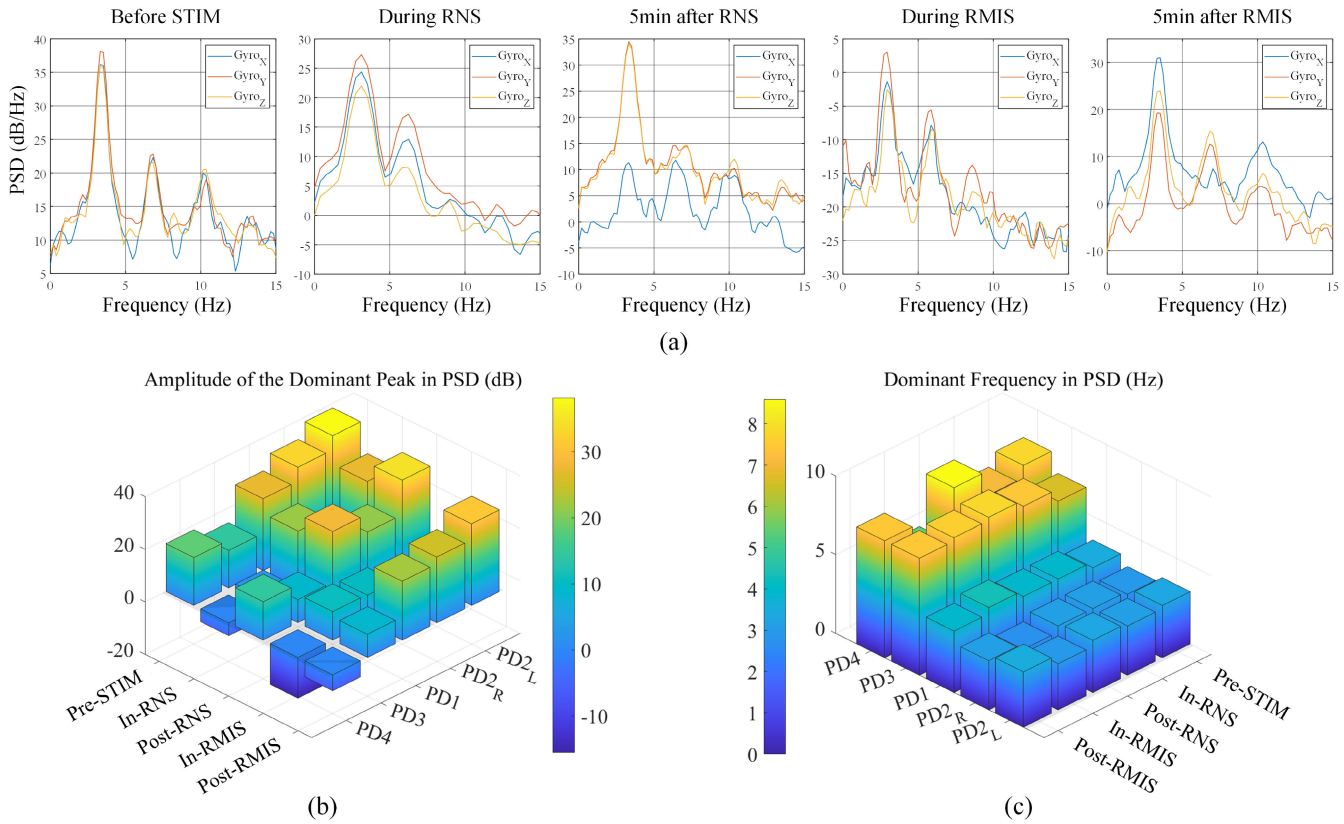

Fig. 8. Original tremor data and frequency characteristics of PD patients before stimulation. The time-frequency characteristics of the original tremor kinematic data were extracted through wavelet analysis, with the frequency domain being represented on a logarithmic scale.

decreased to 3.06 dB/Hz, indicating a substantial reduction in tremor amplitude. Five minutes post-RMIS, the amplitude and frequency of the tremor's dominant peak were 31.01 dB/Hz and 3.52Hz, respectively, indicating that the tremor was still reduced. The clinical trial outcomes from both the RNS and RMIS stimulation strategies demonstrated a decrease in tremor intensity for this patient.

The analysis of tremor data from the remaining patients also demonstrated the effectiveness of electrical stimulation. Based on the analysis results of all data, bar graphs were constructed to detail the peaks and frequencies of tremors, as illustrated in Fig. 8 (b) and (c). The bar charts reveal that, on average, RNS led to a reduction in PSD amplitude by 15.149 dB/Hz from pre-stimulation levels ($p < 0.016$), whereas RMIS showed an even more pronounced decrease in PSD amplitude, averaging 24.176 dB/Hz ($p < 0.017$), indicating a stronger tremor suppression effect.

Notably, there was little variation in the tremor frequencies of patients across different trial phases ($p > 0.3652$), with the exception of patient PD4. During the RMIS phase, PD4's tremor frequency shifted from 7.81Hz to 5.46Hz, accompanied by a significant amplitude reduction to -15.54 dB/Hz. Across the five test groups, the highest tremor peak value recorded for any patient undergoing RMIS did not surpass 10.844 dB/Hz, signifying a substantial tremor suppression.

Radial resting tremors in Parkinson's disease can manifest in various forms, including planar tremors, characterized by movement in a single plane (flexion and extension or radial and ulnar deviation), primarily involving y-axis and z-axis tremor components, and rotational tremors, involving rotational movements around the limb axis (pronation and supination), primarily involving x-axis tremor components. The data from IMUs indicate that tremor signals in different dimensions were reduced, effectively suppressing both planar and rotational tremors.

By calculating the TSR based on the dominant peak in PSD, we derive the attenuation ratio of angular velocity within the tremor frequency band. This measure aligns more closely with the tremor amplitude as intuitively understood. During the RNS treatment, tremor amplitude at the peak frequency in the patient's hand decreased by 48.09% to 94.16%, with the average suppression rate throughout the electrical stimulation process reaching 75.92% ($p < 0.00085$). While most patients experienced a TSR exceeding 85% during RMIS, one patient showed a TSR of only 32.73%, highlighting individual variability in response to electrical stimulation. Across five rounds of RMIS experiments involving four patients, the overall average suppression rate was 82.41% ($p < 0.00285$), slightly outperforming RNS in tremor suppression efficacy.

Significantly, findings from both RNS and RMIS strategies reveal the potential for peripheral electrical stimulation to provide prolonged tremor suppression. PSD estimation indicates that 5 minutes following RNS completion, tremor intensity in all but one patient decreased relative to pre-stimulation levels, showing an average reduction of about 47.29% ($p < 0.01404$). This one patient experienced an 8.84% increase in tremor

intensity compared to before stimulation. Similarly, 5 minutes after concluding RMIS, the tremor's inhibitory effect persisted, with an average intensity reduction of 59.91% from baseline ($p < 0.00259$). No patients in clinical trials reported muscle fatigue. These outcomes affirm that both peripheral electrical stimulation approaches exert a notable suppressive effect on tremors, capable of reducing tremor amplitude for a period post-stimulation.

IV. Discussion

In this research, we developed a constant-current electrical stimulator controlled by FPGA to investigate the use of peripheral electrical stimulation for suppressing resting tremors in Parkinson's disease patients, employing a targeted strategy. Aligning with previous findings on tremor suppression through electrical stimulation [32], [33], our study confirmed the inhibitory impact of peripheral electrical stimulation on resting tremors. Interestingly, our clinical experiments revealed that effective tremor suppression does not solely rely on inducing contractions in the tremor-affected agonist and antagonist muscles. Instead, our findings suggest that applying specific stimulation strategies to nerves or muscles within the tremor's afferent pathway can successfully mitigate tremors at low current intensities while avoiding muscle rigidity. This research suggests potential pathways for the development of wearable tremor suppression devices and helps provide theoretical and practical knowledge for advancing tremor detection sensors, electrical stimulation devices, and stimulation strategies.

Motor neuron dysfunction in Parkinson's disease significantly affects fine motor movements, especially in the fingers and wrists [34]. This study utilizes IMU sensors for precise tremor detection, leveraging the IMU's gyroscope, which accurately measures dynamic movements without gravitational bias. This capability allows for a detailed assessment of tremor severity through angular velocity data. Employing IMUs for tremor detection harnesses their high precision, sensitivity, and portability, ideal for wearable technology. Experiments on Parkinson's patients, with sensors placed on various hand locations, revealed that while tremor frequencies at different joints showed minimal variance, indicating some data overlap, the tremor amplitude was significantly higher at the DIP compared to the CMC and forearm—3.76 and 4.06 times, respectively ($p < 0.0274$). Therefore, positioning IMUs closer to the fingers is recommended to reduce sensor count while boosting detection accuracy and efficiency, an essential strategy for developing cost-effective tremor management solutions.

The FPGA-controlled constant-current electrical stimulator developed in this research enables personalized adjustments for patients by accurately quantifying various stimulation parameters. Especially when implementing the RNS strategy, due to differences in subjective tolerance, the current intensity applicable to different patients (activating the superficial branch of the radial nerve and delivering it to the dorsal digital branch of the radial nerve) may vary up to 12 mA. Moreover, its design incorporates symmetrical bidirectional balanced pulses, essential for balancing electrical stimulation and preventing charge accumulation under the skin. The stimulator's parameter response efficiency has been rigorously tested under both resistive loads and human skin, validating its precision in parameter quantification. With the help of the excellent computing performance of MCU and the driving bottom layer of FPGA, the stimulator can output pulse current in the pulse width output range of $0 \sim 510$us and the frequency of $0 \sim 255$Hz. Additionally, it facilitates real-time and flexible programming of these stimulation parameters via serial communication. This capability is particularly critical for the RMIS strategy, facilitating alternating stimulation of the FCR and ECR electrodes to prevent muscle stiffness. Powered by an H-bridge circuit, it consistently delivers currents from 0 to 60mA across loads of 500 to 5000 ohms, showcasing its versatility across various impedance levels to maintain treatment consistency and effectiveness. Compared with some common programmable electrical stimulation therapy devices, the total weight of this device is only 105 grams when carrying batteries, which is extremely portable and easier to integrate into wearable devices.

When testing the responsiveness of the stimulator, we initially included a wide current output range up to 60 mA to evaluate the maximum capabilities of the device. Recognizing that such high currents are not necessary in a clinical setting, especially for forearm muscle stimulation, we adjusted the discussion to focus on a more clinically relevant range (0-20 mA) and improve the current step accuracy within that range. This adjustment is more consistent with typical therapeutic applications and emphasizes safety.

Our study introduces Co-contraction Avoidance Stimulation (CAS) strategies, which differ from conventional closed-loop methods by focusing on alternating muscle stimulation patterns. This open-loop approach prevents simultaneous contraction of antagonistic muscles, reducing muscle stiffness and discomfort. While closed-loop systems using IMU and EMG provide real-time feedback, our CAS strategies offer a novel, straightforward alternative for initial clinical applications. Future work will incorporate real-time feedback to enhance precision and efficacy.

Preliminary findings demonstrated that a 1 Hz frequency was effective in providing initial tremor suppression and improving patient comfort by reducing the co-contraction of the FCR and ECR muscles. This frequency was intentionally selected to avoid synchronization with the typical 3-8 Hz tremor frequency observed in Parkinson's disease patients. Future studies will investigate various stimulation frequencies within the typical tremor range to optimize efficacy. Our observations revealed significant bilateral differences in tremor manifestations among patients, with varying amplitudes and frequencies between the dominant and non-dominant hands. The dominant hand often exhibited higher tremor amplitude due to greater use and increased neural activity. These findings highlight the need for customized treatment protocols for each hand. The dominant hand may require more intensive or targeted stimulation for optimal suppression. Future studies will focus on developing such tailored protocols to enhance patient outcomes.

While our study shows the potential of the developed stimulator and strategies, there are limitations. The sample size of four patients is small, limiting generalizability. Future research should include a larger cohort. Integrating closed-loop feedback systems could enhance precision and efficacy, and future work will focus on this. The current stimulator design is limited to two channels, expanding them could improve outcomes. Miniaturization and ergonomic improvements are also necessary for better wearability and comfort.

In conclusion, our findings underscore the potential of peripheral electrical stimulation in tremor management. Future research will focus on expanding patient cohorts, integrating closed-loop systems, and improving stimulator design to optimize treatment efficacy and patient comfort.

Our research delves into electrical stimulation strategies aimed at effectively reducing tremors without causing muscle rigidity or fatigue. Diverging from some Functional Electrical Stimulation (FES) approaches that employ high stimulation currents exceeding the MT to induce co-contraction in the ECR and FCR muscles [21], [23], [35], our method does not rely on strong stimulation or synchronize stimulation with muscle activation in response to real-time tremor signals. Instead, we utilize alternating weak currents to target muscles or nerves, aiming to suppress tremors with minimal side effects. Clinical trial results have shown promising outcomes for both stimulation strategies. Through the RNS approach, we observed up to a 75.92% TSR in patients with PD, noting substantial variation in current intensity due to individual differences in electrical stimulation tolerance, with a maximum of 12mA in the RNS strategy. Conversely, trials using the RMIS approach, facilitated by a flexible programmable stimulator, achieved an average TSR of 82.41% with maximum pulse currents below 8mA (average stimulation current of 5.4mA). While patient responses to tremor suppression varied, the overall efficacy of peripheral electrical stimulation in significantly reducing tremors without necessitating muscle contractions was evident. This approach is particularly valuable in maintaining PD patients' adherence to treatment plans by avoiding muscle fatigue, underscoring the potential of tailored electrical stimulation in managing PD symptoms.In conclusion, patients with PD who received peripheral electrical stimulation had a significantly reduced degree of resting tremor compared with before stimulation. Among the two electrical stimulation strategies, the RMIS strategy is more acceptable to PD patients because its current intensity is lower than that of the RNS strategy. Although the stimulation current intensity used by the RMIS strategy is less than the motor threshold that causes muscle contraction, this slight stimulation seems to be enough to affect the muscle's response mechanism to the tremor signal transmitted by the nerve. This finding verifies the potential therapeutic effect of mild electrical stimulation on tremor in PD, and also demonstrates the value of using electrical stimulation devices for daily tremor management in Parkinson's patients. This study contributes to the development of wearable tremor suppression devices that combine detection, identification, and suppression capabilities, promising more efficient and convenient tremor management for PD patients, enhancing their quality of life and broadening treatment possibilities.

V. Conclusion

This paper mainly explores the strategy of using peripheral electrical stimulation to suppress resting tremor in patients with Parkinson's disease. We independently design a multi-parameter programmable electrical stimulator based on FPGA control and conduct clinical trials in PD patients with tremor symptoms. After testing, the electric stimulator has good adjustment capabilities for current intensity, pulse width and frequency parameters, and the constant current stimulation effect is stable. In view of the pathogenesis of resting tremor, this article proposes two electrical stimulation strategies to avoid active and passive co-contraction of antagonistic muscles, respectively targeting the radial nerve and radial muscles of the hand in the tremor pathogenesis. According to the tremor data recorded by the detection sensor in the experiment, the tremor inhibition rate of radial nerve and muscle interference using CAS strategies reached 75.92% and 82.41% respectively, and the inhibitory effect was still achieved 5 minutes after the end of stimulation. At the same time, according to patient feedback, there is basically no fatigue or discomfort during the stimulation process. This article provides a peripheral electrical stimulation solution for relieving resting tremor in PD patients and provides an application reference for the development of wearable tremor suppression devices.

References

[1] B. R. Bloem, M. S. Okun, and C. Klein, "Parkinson's disease," *Lancet*, vol. 397, no. 10291, pp. 2284–2303, Jun. 2021, doi: 10.1016/s0140-6736(21)00218-x.

[2] J. A. Obeso et al., "Past, present, and future of Parkinson's disease: A special essay on the 200th anniversary of the shaking palsy," *Movement Disorders*, vol. 32, no. 9, pp. 1264–1310, Sep. 2017, doi: 10.1002/mds.27115.

[3] M. F. Dirkx and M. Bologna, "The pathophysiology of Parkinson's disease tremor," *J. Neurological Sci.*, vol. 435, Apr. 2022, Art. no. 120196, doi: 10.1016/j.jns.2022.120196.

[4] G. Deuschl et al., "The clinical and electrophysiological investigation of tremor," *Clin. Neurophysiol.*, vol. 136, pp. 93–129, Apr. 2022, doi: 10.1016/j.clinph.2022.01.004.

[5] X. Dong-Chen, C. Yong, X. Yang, S. Chen-Yu, and P. Li-Hua, "Signaling pathways in Parkinson's disease: Molecular mechanisms and therapeutic interventions," *Signal Transduction Targeted Therapy*, vol. 8, no. 1, p. 73, Feb. 2023, doi: 10.1038/s41392-023-01353-3.

[6] K. McFarthing et al., "Parkinson's disease drug therapies in the clinical trial pipeline: 2022 update," *J. Parkinson's Disease*, vol. 12, no. 4, pp. 1073–1082, May 2022, doi: 10.3233/jpd-229002.

[7] H. Zach, M. F. Dirkx, D. Roth, J. W. Pasman, B. R. Bloem, and R. C. Helmich, "Dopamine-responsive and dopamine-resistant resting tremor in Parkinson disease," *Neurology*, vol. 95, no. 11, pp. 1461–1470, Sep. 2020, doi: 10.1212/wnl.0000000000010316.

[8] W. Pirker, R. Katzenschlager, M. Hallett, and W. Poewe, "Pharmacological treatment of tremor in Parkinson's disease revisited," *J. Parkinson's Disease*, vol. 13, no. 2, pp. 127–144, Mar. 2023, doi: 10.3233/jpd-225060.

[9] J. K. Krauss et al., "Technology of deep brain stimulation: Current status and future directions," *Nature Rev. Neurol.*, vol. 17, no. 2, pp. 75–87, Feb. 2021, doi: 10.1038/s41582-020-00426-z.

[10] E. Moro, "Complications of DBS surgery—Insights from large databases," *Nature Rev. Neurol.*, vol. 12, no. 11, pp. 617–618, Nov. 2016, doi: 10.1038/nrneurol.2016.163.

[11] N. P. Fromme, M. Camenzind, R. Riener, and R. M. Rossi, "Design of a lightweight passive orthosis for tremor suppression," *J. NeuroEngineering Rehabil.*, vol. 17, no. 1, p. 47, Dec. 2020, doi: 10.1186/s12984-020-00673-7.

[12] G. Herrnstadt, M. J. McKeown, and C. Menon, "Controlling a motorized orthosis to follow elbow volitional movement: Tests with individuals with pathological tremor," *J. NeuroEngineering Rehabil.*, vol. 16, no. 1, p. 23, Dec. 2019, doi: 10.1186/s12984-019-0484-1.

[13] Y. Kobayashi et al., "Development of a soft exosuit for suppressing essential tremor," *IEEE Trans. Med. Robot. Bionics*, vol. 3, no. 3, pp. 783–790, Aug. 2021, doi: 10.1109/TMRB.2021.3084035.

[14] Y. Matsumoto et al., "Development of an elbow-forearm interlock joint mechanism toward an exoskeleton for patients with essential tremor," in *Proc. IEEE/RSJ Int. Conf. Intell. Robots Syst.* Chicago, IL, USA: IEEE, Sep. 2014, pp. 2055–2062, doi: 10.1109/IROS.2014.6942837.

[15] J. Kim, T. Wichmann, O. T. Inan, and S. P. Deweerth, "A wearable system for attenuating essential tremor based on peripheral nerve stimulation," *IEEE J. Translational Eng. Health Med.*, vol. 8, pp. 1–11, 2020, doi: 10.1109/JTEHM.2020.2985058.

[16] B. S. Arruda, C. Reis, J. J. Sermon, A. Pogosyan, P. Brown, and H. Cagnan, "Identifying and modulating distinct tremor states through peripheral nerve stimulation in parkinsonian rest tremor," *J. NeuroEngineering Rehabil.*, vol. 18, no. 1, p. 179, Dec. 2021, doi: 10.1186/s12984-021-00973-6.

[17] A. Pascual-Valdunciel et al., "Peripheral electrical stimulation to reduce pathological tremor: A review," *J. NeuroEngineering Rehabil.*, vol. 18, no. 1, p. 33, Feb. 2021, doi: 10.1186/s12984-021-00811-9.

[18] S. Dosen et al., "Online tremor suppression using electromyography and low-level electrical stimulation," *IEEE Trans. Neural Syst. Rehabil. Eng.*, vol. 23, no. 3, pp. 385–395, May 2015, doi: 10.1109/TNSRE.2014.2328296.

[19] P. T. Lin et al., "Noninvasive neuromodulation in essential tremor demonstrates relief in a sham-controlled pilot trial," *Movement Disorders*, vol. 33, no. 7, pp. 1182–1183, Jul. 2018, doi: 10.1002/mds.27350.

[20] A. Pascual-Valdunciel, A. Rajagopal, J. L. Pons, and S. Delp, "Noninvasive electrical stimulation of peripheral nerves for the management of tremor," *J. Neurological Sci.*, vol. 435, Apr. 2022, Art. no. 120195, doi: 10.1016/j.jns.2022.120195.

[21] E. H. Copur, C. T. Freeman, B. Chu, and D. S. Laila, "Repetitive control of electrical stimulation for tremor suppression," *IEEE Trans. Control Syst. Technol.*, vol. 27, no. 2, pp. 540–552, Mar. 2019, doi: 10.1109/TCST.2017.2771327.

[22] L. Meng, M. Jin, X. Zhu, and D. Ming, "Peripherical electrical stimulation for parkinsonian tremor: A systematic review," *Frontiers Aging Neurosci.*, vol. 14, Feb. 2022, Art. no. 795454, doi: 10.3389/fnagi.2022.795454.

[23] C. T. Freeman, P. Sampson, J. H. Burridge, and A.-M. Hughes, "Repetitive control of functional electrical stimulation for induced tremor suppression," *Mechatronics*, vol. 32, pp. 79–87, Dec. 2015, doi: 10.1016/j.mechatronics.2015.10.008.

[24] Z. Habibollahi, Y. Zhou, M. E. Jenkins, S. J. Garland, M. D. Naish, and A. L. Trejos, "Multimodal tremor suppression of the wrist using FES and electric motors—A simulation study," *IEEE Robot. Autom. Lett.*, vol. 8, no. 11, pp. 7543–7550, Nov. 2023, doi: 10.1109/LRA.2023.3316607.

[25] M.-Z. Hao et al., "Inhibition of parkinsonian tremor with cutaneous afferent evoked by transcutaneous electrical nerve stimulation," *J. NeuroEngineering Rehabil.*, vol. 14, no. 1, p. 75, Dec. 2017, doi: 10.1186/s12984-017-0286-2.

[26] A. Pascual-Valdunciel et al., "Intramuscular stimulation of muscle afferents attains prolonged tremor reduction in essential tremor patients," *IEEE Trans. Biomed. Eng.*, vol. 68, no. 6, pp. 1768–1776, Jun. 2021, doi: 10.1109/TBME.2020.3015572.

[27] J. Liu, S. Qu, Z. Suo, and W. Yang, "Functional hydrogel coatings," *Nat. Sci. Rev.*, vol. 8, no. 2, Feb. 2021, Art. no. nwaa254, doi: 10.1093/nsr/nwaa254.

[28] P. Y. Chan et al., "Motion characteristics of subclinical tremors in Parkinson's disease and normal subjects," *Sci. Rep.*, vol. 12, no. 1, p. 4021, Mar. 2022, doi: 10.1038/s41598-022-07957-z.

[29] J. V. D. Wardt et al., "Systematic clinical approach for diagnosing upper limb tremor," *J. Neurol., Neurosurgery Psychiatry*, vol. 91, no. 8, pp. 822–830, Aug. 2020, doi: 10.1136/jnnp-2019-322676.

[30] E. Tolosa, A. Garrido, S. W. Scholz, and W. Poewe, "Challenges in the diagnosis of Parkinson's disease," *Lancet Neurol.*, vol. 20, no. 5, pp. 385–397, May 2021, doi: 10.1016/s1474-4422(21)00030-2.

[31] S. Ancona et al., "Wearables in the home-based assessment of abnormal movements in Parkinson's disease: A systematic review of the literature," *J. Neurol.*, vol. 269, no. 1, pp. 100–110, Jan. 2022, doi: 10.1007/s00415-020-10350-3.

[32] Z. Hu, S. Xu, M. Hao, Q. Xiao, and N. Lan, "The impact of evoked cutaneous afferents on voluntary reaching movement in patients with Parkinson's disease," *J. Neural Eng.*, vol. 16, no. 3, Jun. 2019, Art. no. 036029, doi: 10.1088/1741-2552/ab186f.

[33] J. Kim, T. Wichmann, O. T. Inan, and S. P. DeWeerth, "Analyzing the effects of parameters for tremor modulation via phase-locked electrical stimulation on a peripheral nerve," *J. Personalized Med.*, vol. 12, no. 1, p. 76, Jan. 2022, doi: 10.3390/jpm12010076.

[34] M. J. Armstrong and M. S. Okun, "Diagnosis and treatment of Parkinson disease: A review," *JAMA*, vol. 323, no. 6, p. 548, Feb. 2020, doi: 10.1001/jama.2019.22360.

[35] F. Widjaja, C. Y. Shee, W. L. Au, P. Poignet, and W. T. Ang, "Using electromechanical delay for real-time anti-phase tremor attenuation system using functional electrical stimulation," in *Proc. IEEE Int. Conf. Robot. Autom.*, Shanghai, China, May 2011, pp. 3694–3699, doi: 10.1109/ICRA.2011.5979865.